Chemical Science

ROYAL SOCIETY OF CHEMISTRY

EDGE ARTICLE

View Article Online
View Journal | View Issue

Cite this: *Chem. Sci.*, 2020, **11**, 3737

All publication charges for this article have been paid for by the Royal Society of Chemistry

Inhibiting cancer metabolism by aromatic carbohydrate amphiphiles that act as antagonists of the glucose transporter GLUT1†

Alexandra Brito, [abcd] Patrícia M. R. Pereira, [c] Diana Soares da Costa, [ab] Rui L. Reis, [abe] Rein V. Ulijn, [dfg] Jason S. Lewis, [chijk] Ricardo A. Pires *[abe] and Iva Pashkuleva *[ab]

We report on aromatic *N*-glucosides that inhibit selectively the cancer metabolism *via* two coexistent mechanisms: by initial deprivation of the glucose uptake through competitive binding in the glucose binding pocket of GLUT1 and by formation of a sequestering nanoscale supramolecular network at the cell surface through localized (biocatalytic) self-assembly. We demonstrate that the expression of the cancer associated GLUT1 and alkaline phosphatase are crucial for the effectiveness of this combined approach: cancer cells that overexpress both proteins are prompter to cell death when compared to GLUT1 overexpressing cells. Overall, we showcase that the synergism between physical and biochemical deprivation of cancer metabolism is a powerful approach for development of effective anticancer therapies.

Received 15th February 2020
Accepted 9th March 2020

DOI: 10.1039/d0sc00954g

rsc.li/chemical-science

Introduction

Cancer is a major health problem for modern society, causing 9.6 million deaths worldwide in 2018 and the 5 year prevalence was estimated to be 43.8 million.[1] These statistics show that the conventional therapies are not sufficiently effective. There are two main reasons that limit the efficacy of existing treatments - the great complexity and consequent limited understanding of cancer cells, and their resistance to the currently used therapeutics.[2–4] Common strategies for targeting the inhibition of specific molecular pathways often have only temporary success followed by a tumor relapse.[4] The use of a combined approach with several drugs can give rise to higher efficiency and avoidance of chemoresistance but so far, the results did not achieve the required efficacy.[2] Herein, we propose an alternative approach to cancer management that uses a single, multifunctional but yet specific molecule that targets a common cancer hallmark – their accelerated metabolism associated with a higher demand for nutrients and energy – *via* two synergistic pathways, namely by formation of a nanoscale supramolecular

[a]*3B's Research Group, I3Bs – Research Institute on Biomaterials, Biodegradables and Biomimetics, University of Minho, Headquarters of the European Institute of Excellence on Tissue Engineering and Regenerative Medicine, AvePark, Parque de Ciência e Tecnologia, Zona Industrial da Gandra, 4805-017 Barco, Guimarães, Portugal. E-mail: rpires@i3bs.uminho.pt; pashkuleva@i3bs.uminho.pt*

[b]*ICVS/3Bs – PT Government Associate Laboratory, Braga/Guimarães, Portugal*

[c]*Department of Radiology, Memorial Sloan Kettering Cancer Center, New York, NY 10065, USA*

[d]*Advanced Science Research Center (ASRC) at the Graduate Center, City University of New York (CUNY), 85 St Nicholas Terrace, New York, New York 10031, USA*

[e]*The Discoveries Centre for Regenerative and Precision Medicine Headquarters at University of Minho, Avepark, 4805-017 Barco, Guimarães, Portugal*

[f]*Department of Chemistry, Hunter College, City University of New York, 695 Park Avenue, New York 10065, USA*

[g]*PhD Programs in Biochemistry and Chemistry, The Graduate Center of the City University of New York, New York 10016, USA*

[h]*Department of Radiology, Weill Cornell Medical College, New York, NY 10065, USA*

[i]*Molecular Pharmacology Program, Memorial Sloan Kettering Cancer Center, New York, NY 10065, USA*

[j]*Department of Pharmacology, Weill Cornell Medical College, New York, NY 10065, USA*

[k]*Radiochemistry and Molecular Imaging Probes Core, Memorial Sloan Kettering Cancer Center, New York, NY 10065, USA*

† Electronic supplementary information (ESI) available. See DOI: 10.1039/d0sc00954g

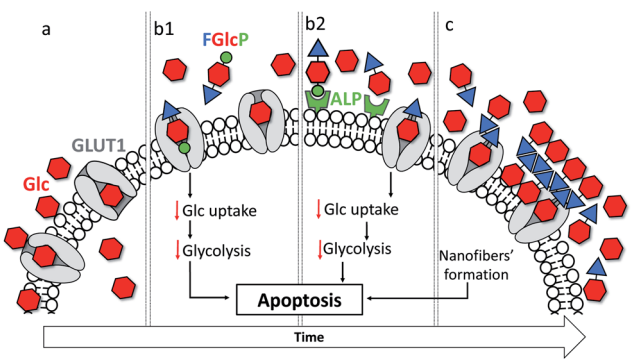

Fig. 1 Schematic presentation of the mechanism of action of *N*-fluorenylmethyloxycarbonyl-glucosamine-6-phosphate (FGlcP): (a) the increased glucose (Glc) metabolism is targeted *via* concomitant (b) blocking of the overexpressed glucose transporters (GLUT1) with (b1) FGlcP or/and (b2) its dephosphorylated analogue generated *in situ* and (c) formation of nanonet by self-assembly of this analogue.

network around cancer cells and by the blockage of glucose transportation (Fig. 1).[4,5]

The altered cancer metabolism has inspired the development of various therapies.[6–11] Among them, biocatalytic self-assembly (BSA) has emerged as a biochemical approach that makes use of pathologically overexpressed enzymes (typically MMPs or phosphatases) to transform specifically designed precursors into self-assembling molecules and to trigger their assembly *in situ*, *i.e.* in close proximity of cancer cells.[2,6,12–20] Several studies suggested a mechanism that involves an initial internalization of the precursor by the cells, followed by intracellular enzymatic transformation and assembly that leads to cellular death.[6,18,21] Most of the described precursors are based on short self-assembling peptides that are functionalized with enzymatic sensitive moieties.[11,12,17,19–21] We recently demonstrated the use of a glucose derivative, *N*-fluorenylmethyloxycarbonyl-glucosamine-6-phosphate (FGlcP), as an alternative to peptide-based systems in phosphatase-triggered BSA cancer management.[7] For this system, we did not observe any intracellular assembly but formation of a nanoscale supramolecular network around osteosarcoma cells that overexpress membrane-bound alkaline phosphatase (ALP). The system proved to be effective in killing osteosarcoma cells. The amphiphile structure is based on glucose (Glc), which led us to hypothesize that FGlcP might act not only as a BSA precursor but also as an antagonist of the Glc transport, inhibiting aerobic glycolysis. Herein we investigate this hypothesis and demonstrate that a single compound, FGlcP, acts as an efficient cancer antimetabolite by concomitant blocking the glucose transporter 1 (GLUT1) *via* specific interactions with them and formation of a nanonet serving not only as a physical barrier between the cancer cells and their environment, but also as a reservoir of GLUT inhibitor (Fig. 1).

Results

Molecular design and synthesis of aromatic *N*-glucosides

We designed and synthesized three derivatives (Fig. 2) of Glc (**1a**) aiming to establish reliable controls and to investigate the influence of different functional components (aromatic, glucose, charged groups) in the interactions with GLUT1. FGlcP (**1b**) is a BSA precursor that is transformed into the self-assembling molecule *N*-fluorenylmethyloxycarbonyl-glucosamine (FGlc, **1c**) upon phosphatase action (Fig. 1(b2)).[7]

FGlc does not contain a charged group and thus, it has reduced solubility in aqueous media. Previously, we have shown that **1c** can self-assemble into nanofibers above a critical concentration that can be achieved upon heating or enzymatic action.[7,22,23] *N*-fluorenylmethyloxycarbonyl glucosamine-6-sulphate (FGlcS, **1d**) is an analogue of FGlcP, in which the phosphate group is replaced by a negatively charged sulphate. From a mechanistic point of view, the main difference between **1b** and **1d** is that the sulfate derivative is not susceptible to phosphatase transformation and the subsequent self-assembly (Fig. S4†), *i.e.* we hypothesize that it will act solely as GLUT1 antagonist. All compounds were synthesized using a previously established procedure.[7,22,23]

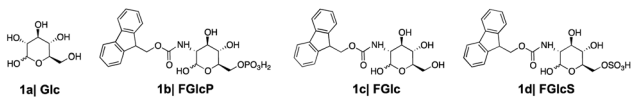

Fig. 2 Glucose (**1a**) and aromatic *N*-glucosides (**1b–d**) synthesized and used in this study.

In silico analysis shows that 1a–d bind to GLUT1

Overexpression of GLUT1 has been associated with different tumor types.[9,10,24] We evaluated the differential interactions of the compounds **1a–d** with GLUT1 by a computational molecular-docking process using the web-based SwissDock program (Tables 1 and S1†).[25,26] The parameters were set for blind docking, *i.e.* we did not define *a priori* any specific region for binding. Docking studies with Glc (**1a**) were also carried out using these parameters to confirm the fidelity of the generated outputs by comparison with published data.[8,27,28] The results demonstrated spontaneous complexation between GLUT1 and all compounds **1a–d**: Gibbs free energy for all studied systems was negative ($\Delta G < 0$) but the absolute values are larger for the amphiphiles **1b–d** when compared to **1a** (Table 1), indicating a higher affinity of these derivatives to the transporter. Van der Waals interactions (ΔG_{vdw}) have the greatest contribution to this spontaneous process (*InterFull* values are the same as ΔG_{vdw}) especially in the case of aromatic *N*-glucosides (**1a** *vs.* **1b–d**) suggesting involvement of additional π–π and CH–π interactions due to the introduced Fmoc functionality. Modification with polar groups reduces additionally the ΔG_{vdw} (**1c** *vs.* **1b** and **1d**) but also the solvation energy ($\Delta G_{ligsolvpol}$) evidencing formation of H-bonding between the GLUT1 and phosphate (**1b**) or sulfate (**1d**) groups. Of note, all compounds **1a–d** bind to the same pocket *via* interactions with amino acids that are crucial for the Glc complexation with GLUT1 (Fig. 3 and Table S1†).[8,27,28] Altogether the *in silico* data indicated that the studied compounds can deprive the Glc transport *via* competitive binding to GLUT1 and their antagonist activity follows the order: **1b** > **1d** > **1c**.

Selection of cancer cell lines

To test the effect of the aromatic carbohydrate amphiphiles we selected an osteosarcoma cell line (SaOs2) and a mammary gland/breast cancer cell line (MDA-MB-468) based on an initial search in the Cancer Cell Line Encyclopedia (CCLE) for cell lineages with high expression of solute carrier family 2 member 1 gene (*SLC2A1*) encoding GLUT1.[29,30] We confirmed the expression of GLUT1 in SaOs2 and MDA-MB-468 cancer cells at transcriptional and protein levels (Fig. S5†).

PCR analysis demonstrated that the selected cell lines express the *SLC2A1* gene (Fig. S5a†). Immunostaining confirmed the expression of GLUT1 for both cell lines (Fig. S5b†) but flow cytometry analysis demonstrated 2-fold larger population of cells expressing GLUT1 in SaOs2 compared with MDA-MB-468 (Fig. S5c†). In addition, SaOs2 overexpress membrane-bound alkaline phosphatase that can trigger BSA on their surface while MDA-MB-468 present 3-fold less expression of this enzyme (Fig. S5d†).[7] These differences are important for the experimental design as they might enable us to distinguish

Table 1 *In silico* predictions for the binding energies involved in the interactions between GLUT1 and glucose (**1a**) or its derivatives (**1b–d**). The results were obtained from top score models generated with SwissDock[a]

Comp	ΔG (kcal mol^{-1})	ΔG_{vdw} (kcal mol^{-1})	$\Delta G_{ligsolvnonpol}$ (kcal mol^{-1})	$\Delta G_{ligsolvpol}$ (kcal mol^{-1})
1a	−6.77	−36.32	6.48	−13.50
1b	−10.09	−68.89	10.36	−24.31
1c	−8.33	−44.94	9.39	−16.74
1d	−9.04	−55.70	10.57	−23.14

[a] ΔG: Gibbs energy; ΔG_{vdw}: energy of van der Waals interactions; $\Delta G_{ligsolvnonpol}$: solvation energy due to non-polar interactions; $\Delta G_{ligsolvpol}$: solvation energy due to polar interactions.

the two possible mechanisms by which the amphiphiles can affect the metabolism of the cancer cells – BSA and inhibition of GLUT1 as well as any cooperative effect between these mechanisms.

Aromatic *N*-glucosides decrease Glc uptake by tumor cells

We used 2-(*N*-(7-nitrobenz-2-oxa-1,3-diazol-4-yl)amino)-2-deoxyglucose (**NBDG**) for visualization and quantification of the cells' glucose uptake in the presence and absence of compounds **1b–d**.[31,32] Initially, the rate of **NBDG** uptake was studied for different incubation periods and concentrations using previously established protocols.[31,33] A maximal fluorescence (indicating maximal **NBDG** uptake) was observed when cells were cultured in medium supplemented with 0.02 mM **NBDG** for 30 min, which were the conditions used below.

We designed a competitive assay in which the selected cell lines were incubated with **NBDG** in the presence of one of the

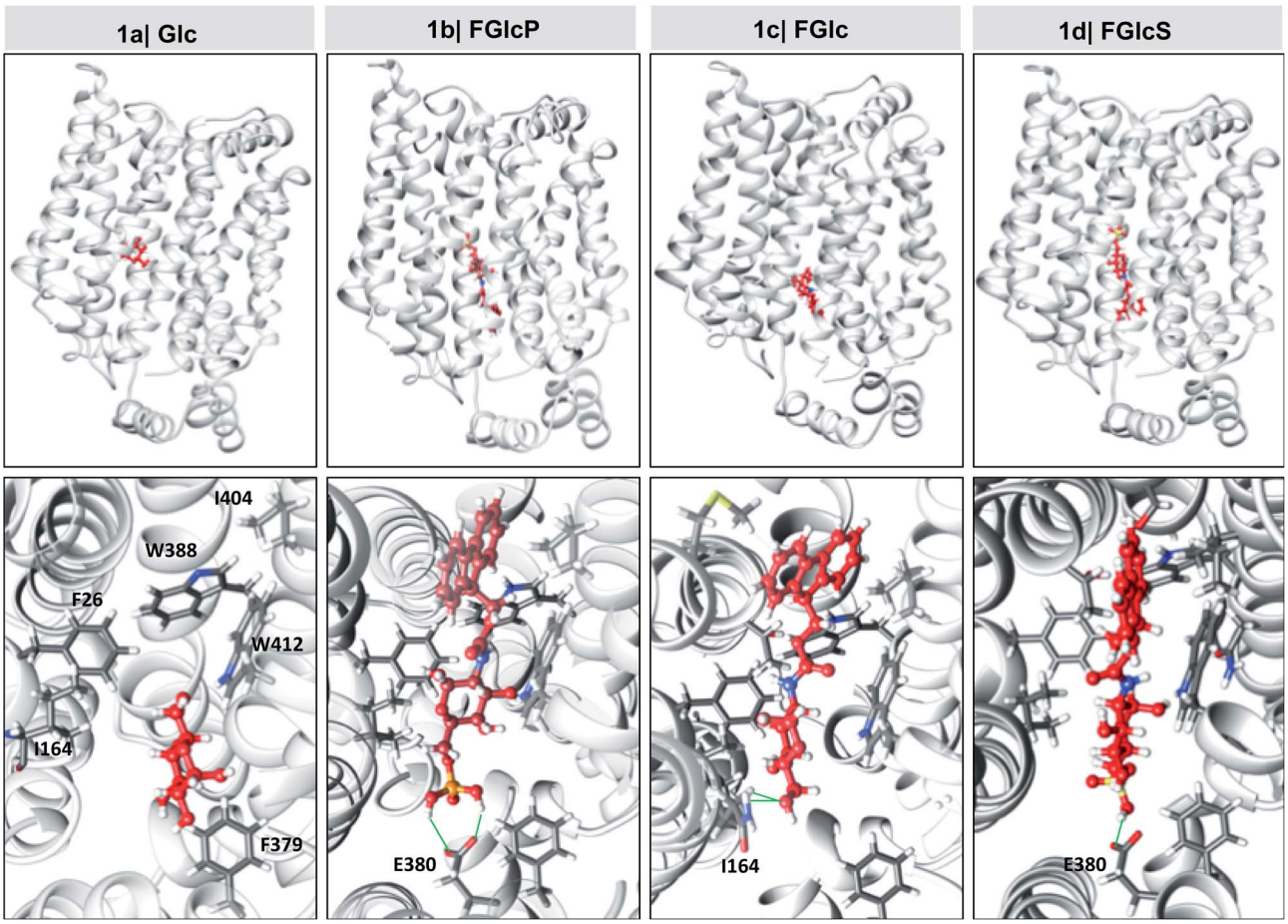

Fig. 3 *In silico* models for the interactions between the synthesized aromatic *N*-glucosides (**1b–d**, red) and GLUT1 (grey). The upper row shows top score clusters (with the lowest *FullFitness*) of the full-size complex where the extracellular segment of GLUT1 is oriented upwards and the intracellular one downwards. The bottom row represents the magnification of the glucose-binding pocket in GLUT1. Hydrogen bonds are denoted with green lines.

compounds **1b–d**, *i.e.* conditions at which **NBDG** will compete with the aromatic *N*-glucosides for GLUT1. We observed that significantly less **NBDG** was taken up by both of the tested cell lines (Fig. 4) suggesting that **1b–d** act as GLUT1 antagonists, in agreement with the *in silico* models. To demonstrate whether this approach is applicable in clinically relevant scenario, we also performed molecular imaging with the clinically established fluorodeoxyglucose (^{18}F-FDG) positron emission tomography (PET). Our results showed that PET is suitable for monitoring the effect of the aromatic *N*-glucosides on the Glc distribution *in vivo* and we observed deprivation of the **NBDG** uptake at the tumor site upon supplementation with **1b** (Fig. S6†).

The effect of the aromatic *N*-glucosides is mediated by GLUT1

GLUT1 expression was quantified by western blot analysis (Fig. 5a). We performed cell surface biotinylation to distinguish GLUT1 expressed at the cell surface and responsible for the Glc uptake from the total GLUT1 expression. The results demonstrated that cancer cells' incubation with aromatic *N*-glucosides significantly reduces the transporter expression on the cell surface but does not affect the total GLUT1 expression (Fig. 5a). These data agree with the formation of a strong complex between the aromatic *N*-glucosides and GLUT1 with consecutive blockage of the transporter (Fig. 5d). Further confirmation of this mechanism of action was derived by *SLC2A1* knockdown. We used a pool of three target-specific nucleotides 19–25 (nt) small-interfering RNA (siRNA). A maximal *SLC2A1* suppression (>50%) was observed 48 h after post-transfection for the SaOs2 cells (Fig. 5b) and 24 h for the MDA-MB-468 (Fig. S7†). The transfected cells displayed a markedly decreased sensitivity to the compounds **1b–d** confirming that their activity is mediated by GLUT1 (Fig. 5c).

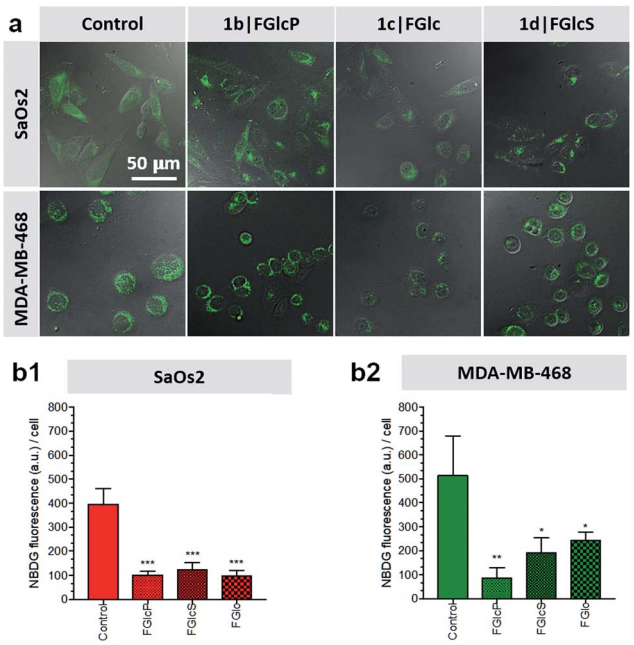

Fig. 4 Aromatic *N*-glucosides **1b–d** block glucose uptake by tumor cells: (a) representative fluorescent confocal scanning microscopy images showing uptake of 2-(*N*-(7-nitrobenz-2-oxa-1,3-diazol-4-yl) amino)-2-deoxyglucose (**NBDG**, green) by the SaOs2 and MDA-MB-468 cancer cells in the presence of aromatic *N*-glucosides **1b–d**: cells were incubated with 0.02 mM of **NBDG** in the presence of 0.5 mM of the aromatic *N*-glucoside and visualized after 30 min; (b) **NBDG** uptake calculated from the fluorescence images; statistics were calculated using the *t*-test *: $p < 0.05$; **: $p < 0.01$; ***$p < 0.001$.

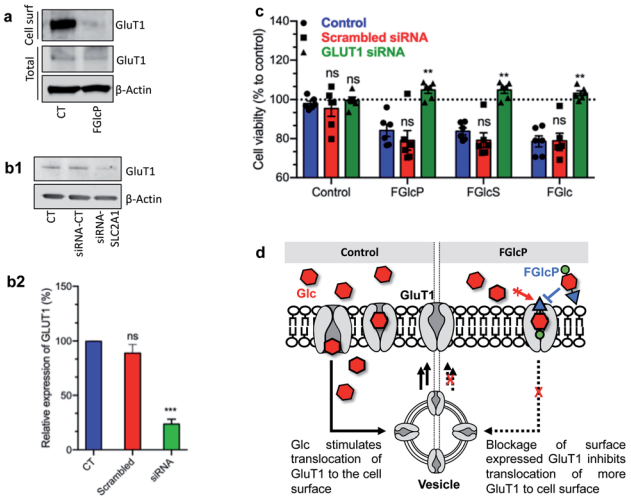

Fig. 5 Influence of GLUT1 expression on the effect of aromatic *N*-glucosides on SaOs2 viability. (a) Representative western blot analysis showing changes in GLUT1 expressed on the cell surface (extracts obtained by cell-surface biotinylation) and the total GLUT1 in SaOs2 cells without (CT) and with supplementation of **1b**. (b1) Representative western blot analysis and (b2) the respective densitometric analysis of GLUT1 expression by SaOs2 cells without transfection (CT) and after transfection with scrambled siRNA (siRNA-CT) or specific GLUT1 siRNA (siRNA-SLC2A1); (c) cell viability of the transfected SaOs2 cells after incubation with 0.5 mM aromatic *N*-glucosides **1b–d** for 1 h (quantification was performed after 24 h). (d) Schematic presentation of the GLUT1 transduction role. *ns*, non-significant; **$p < 0.05$; ***$p < 0.001$. Data for MDA-MB-468 are provided in Fig. S3.†

Concomitant saturation binding experiments using **NBDG** at different concentrations without and in the presence of the respective aromatic *N*-glucosides were performed to determine the dissociation constant ($K_{d\ NBDG}$) and the number of the binding sites (B_{max}) for each cell line (Table 2 and Fig. S8†).

The results supported the proposed mechanism (Fig. 5d) and showed that supplementation with **1b–d** decreased the expression of GLUT1 on the cell surface (B_{max}, Table 2) and the **NBDG** binding by GLUT1 ($K_{d\ NBDG}$, Table 2). Of note, the used method does not allow comparison of the obtained $K_{d\ NBDG}$ (defined as a concentration at which **NBDG** binds to half of the available GLUT1) for SaOs2 and MDA-MB-468 cells because of the different B_{max} values but the effect of **1b–d** on each cell line can be compared (similar B_{max}).[34] For SaOs2 cells, we obtained the smallest $K_{d\ NBDG}$ in the presence of **1b** which means that this *N*-glucosamine blocks more efficiently the GLUT1 on the cell surface and less **NBDG** is needed to saturate the available GLUT1. In the case of MDA-MB-468 cells, the smallest $K_{d\ NBDG}$ was obtained for the **1d**.

Table 2 Number of GLUT1 (B_{max}) and dissociation constants ($K_{d\ NBDG}$) for SaOs2 and MDA-MB-468 determined by concomitant saturation binding experiments for **NBDG** in the presence of aromatic *N*-glucosides **1b–d** (0.5 mM). The respective curves are presented in Fig. S8

Cells	Comp	B_{max} (GLUT1/cell × 10^8)	$K_{d\ NBDG}$ (μM)
SaOs2	**NBDG**	1.70	0.99
	1b	0.75	0.14
	1c	0.58	0.32
	1d	0.76	0.38
MDA-MB-468	**NBDG**	3.80	0.28
	1b	2.42	0.19
	1c	2.73	0.16
	1d	2.80	0.11

N-glucosides-mediated GLUT1 inhibition leads to cell death *via* an apoptotic mechanism

We observed that cancer cells incubated with the compounds **1b–d** have lower metabolic activity and cell proliferation, leading to an overall decrease in cell survival over time (Fig. 6a, S9 and S10†). This effect was not observed for prechondrocyte ATDC5 cells, which remained viable and proliferated in the presence of **1b** and **1d** (Fig. S11†).

Confirmation that this response is due to the GLUT1 inhibition and consecutive deprivation of the Glc uptake was obtained by quantification of the lactate production in the studied cells. Lactate is the last metabolite of glycolysis in cancer cells and indeed, its production was significantly inhibited (>60%) by treatment with **1b** (Fig. 6b). We also investigated the type of cell death induced by this treatment. We studied the effect of **1b–d** in a presence of an apoptosis (Z-Fa-FMK) or a necroptosis (Nec-1) inhibitor.[35,36] We observed that Z-Fa-FMK rescues the SaOs2 and MDA-MB-468 cells treated by **1b–d** (Fig. 6c) while the addition of Nec-1 has no effect on cell survival (Fig. S12†). These results demonstrate that the aromatic *N*-glucosides activate apoptotic pathways in the cells overexpressing GLUT1. This result was also confirmed by the expression of the apoptosis-associated caspases 8 and 9.[37,38] Caspases are initially produced as inactive monomeric procaspases that require dimerization and often cleavage for activation.[38] We found that the apoptosis pathways are activated by cleavage of procaspase 8 (53 kDa) to shorter motifs (43 kDa, 18 kDa) and procaspase 9 (47 kDa) to oligomers of 25 kDa (Fig. S13†).

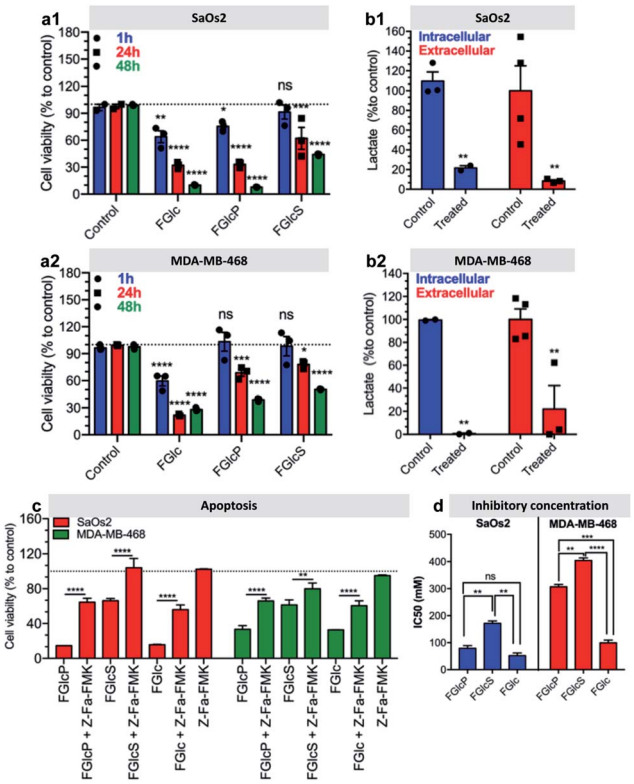

Fig. 6 Aromatic *N*-glucosides deprive glycolysis and induce cell death. (a) Viability of (a1) SaOs2 and (a2) MDA-MB-468 cells after different incubation times with 0.5 mM **1b–d**; (b) intra- and extracellular lactate production by (b1) SaOs2 and (b2) MDA-MB-468 cells prior and after treatment with **1b**; (c) effect of the apoptosis inhibitor Z-Fa-FMK on cell viability (24 h) in the presence of the compounds **1b–d** (0.5 mM); (d) inhibitory concentrations of the studied *N*-glucosides determined for SaOs2 and MDA-MB-468 (24 h). All results are normalized to the control – cell culture without aromatic *N*-glucosides. *ns* statistically non-significant difference; *$p < 0.05$; **$p < 0.01$; ***$p < 0.001$; ****$p < 0.0001$.

Discussion

Cancer cells have a high energy demand that is associated with an increased glucose uptake (Warburg effect) and overexpression of glucose transporter proteins (GLUTs). The elevated consumption of Glc assures an immediate production of adenosine triphosphate, but also increases the availability of biosynthetic intermediates that support the highly proliferative nature of cancer cells.[39–41] As a result, cancer cells are very sensitive to Glc deprivation, which can prevent proliferation and induce cell death.[41] Glc is delivered inside cancer cells *via* the GLUTs, among which GLUT1 is upregulated in most of the solid tumours.[9,10,41] GLUTs are therefore suitable targets for the treatment of different types of cancers. Herein, we designed and synthetized several aromatic *N*-glucosides **1b–d** and investigated their potential to deprive the glycolysis in cancer cells. The molecular design of **1b–d** combines several functional elements: the aromatic Fmoc-functionality, which provides amphiphilic character and possibility for self-assembly *via* π–π interactions and the Glc portion that can participate in H-bonding and CH–π interactions and attribute GLUT antagonist characteristics are common features for all studied compounds. FGlc (**1c**) that contains only these two functional moieties has poor solubility in aqueous media (dimethyl sulfoxide at a concentration below 0.005% was used as a co-solvent). Thus, negatively charged polar group were incorporated within the structure of **1c** generating **1b** and **1d** aiming to improve their water solubility. The polar phosphate group of **1b** imparts also enzyme sensitivity: FGlcP (**1b**) is a BSA precursor that generates the self-assembling FGlc (**1c**) upon ALP action (Fig. 1b) causing cell death by formation of a pericellular supramolecular nanonet (Fig. 1c and S4†).[7,17]

In silico studies confirmed that all aromatic *N*-glucosides **1b–d** bind to the Glc pocket. The significant decrease in ΔG_{vdw} for these compounds when compared to Glc (**1a**) indicate that the aromatic portion (Fmoc) can interact *via* CH–π and π–π interactions with the aromatic rings of *e.g.* Trp388 and Phe26 in the glucose-binding pocket causing conformational changes that can disturb the GLUT1 function (the inward opening, Fig. S14†).[27,28] On the other hand, the lower ΔG of the compounds **1b–d** indicates that even if the inward opening is not compromised, they might not be released because of the strong bonds formed with the GLUT1.

The effect of the aromatic *N*-glucosides on Glc transport was studied *in vitro* using two human cancer cell lines. Because SaOs2 cells express on their surface both ALP and GLUT1 proteins, it is challenging to distinguish the effect of BSA, triggered by ALP *versus* the GLUT1 antagonist effect of **1b–c**. We and others previously demonstrated that BSA is a time and concentration (both enzyme and precursor) dependent process - short incubation times and low concentrations result in formation of very sparse and thus likely permeable supramolecular nanoscale network (Fig. S4†).[7,42] Thus, we have selected one additional human cancer cell line, MDA-MB-468 that expresses 3-fold less ALP on their surface (Fig. S5†). We have also shortened the experimental time to 30 min and lowered the concentration of the aromatic *N*-glucosides to 0.5 mM (*versus* 7 h and 1 mM when the significant effect of BSA on cell viability was observed[7]) aiming to avoid BSA of **1b** and to determine the GLUT1 antagonist effect of the aromatic *N*-glucosides. As in a previous study, we have used ATDC5 prechondrocytes for comparative purposes, *i.e.* to demonstrate the specificity of the aromatic *N*-glucosides towards cancer cells (Fig. S11†).[7] At the studied conditions (30 min, 0.5 mM concentration of *N*-glucosides), we observed very similar response by the two cancer cell lines: the compounds **1b–d** inhibit Glc transport in SaOs2 and MDA-MB-469 (Fig. 4), while ATDC5 were not affected (Fig. S11†). This response was directly related with the GLUT1 expression: viability of SaOs2 and MDA-MB-468 with depleted GLUT1 was not affected by the aromatic *N*-glucosides similarly to ATDC5 that do not express GLUT1 on the surface. It is expected that the reduction of the Glc uptake will result in the translocation of more GLUT1 to the cell membrane.[41] Surprisingly, we observed exactly the opposite effect (Fig. 4a, B_{max} in Table 2). The decrease of GLUT1 translocation to the membrane is indicative about the mechanism of action: GLUT1 proteins bind the aromatic *N*-glucosides but do not release them intracellularly, *i.e.* it is in a permanent ON mode and thus does not mediate correctly the need of Glc (Fig. 4 and S14B†). As a result, cells do not respond to the Glc deprivation because they cannot sense it *via* GLUT1. Another indicative result about the mechanism of action is the obtained $K_{d\ NBDG}$ (Table 2) and IC_{50} values (Fig. 6d and S9†). $K_{d\ NBDG}$ were determined 30 min after supplementation of **1b–d** and showed that in the case of MDA-MB-468 the sulphated **1d** is the most efficient GLUT1 antagonist. Different result was obtained for SaOs2: lowest $K_{d\ NBDG}$ were obtained for **1b** that act simultaneously as a GLUT1 antagonist and as a substrate for biocatalytic self-assembly locally, *i.e.* at the cell surface where ALP is located, thus creating a physical barrier. **1c** can self-assemble too but it forms bulk (throughout the solution) and not local (on the cell surface) nanonet and thus, longer time (or higher concentration) is needed to achieve the same blocking efficacy.

Indeed, the IC_{50} values determined after 24 h of cells exposition to **1b–d**, were lowest for the self-assembling FGlc (**1c**) either for SaOs2 or for MDA-MB-468 cells. A similarly low value was obtained for **1b** but only for SaOs2 cells confirming the above-mentioned mechanism, *i.e.* that the precursor **1b** is already transformed by the ALP of SaOs2 into **1c** and a nanonet is generated around SaOs2 cells.[7] Because MDA-MB-468 cells have lower expression of ALP this transformation does not occur and the IC_{50} value of **1b** is 4-fold higher for these cells. **1d** that is solely involved in the GLUT1 blocking because does not self-assemble into nanofibers (Fig. S4†)[22] and is not susceptible to BSA presented the highest IC_{50} values for both cell lines. These results demonstrate that the formation of a nanonet around the cells not only sequesters them, but also add the inhibitory effect of the aromatic *N*-glucosides most probably by maintaining these compounds at high concentration in the pericellular space, *i.e.* close to GLUT1. In such scenario, the self-assembling **1c** has the greatest effect but its application can be hampered by the poor solubility in aqueous media. The precursor **1b** is an excellent alternative for tumors that overexpress phosphatases on their surface. Besides having the same activity as **1c**, it uses two molecular targets (ALP and GLUT1), thus enhancing its selectivity.

Conclusions

Our study demonstrates that the aromatic *N*-glucosides **1b** and **1d** have a potent anticancer activity due to their ability to inhibit Glc transportation and GLUT1 expression *via* two synergistic physical and biochemical mechanisms: blockage of GLUT1 (**1b** and **1d**) and/or formation of a supramolecular net around the cells (**1b**).

Ethical statement

The animal experiments in this study were performed in strict accordance with the guidelines for the care and use of laboratory animals and approved by the Institutional Animal Care and Use Committee of Memorial Sloan Kettering Cancer Center (NY, USA).

Conflicts of interest

There are no conflicts to declare.

Acknowledgements

We acknowledge the EU's H2020 program (Forecast 668983; THE DISCOVERIES CTR 739572) and the Portuguese FCT (BD/113794/2015; BPD/85790/2012; PTDC/NAN-MAT/28468/2017 CANCER_CAGE) for the financial support. The authors gratefully acknowledge members of the MSKCC Small Animal Imaging Core Facility, the Radiochemistry and Molecular Imaging Probe Core (both supported by NIH P30 CA008748) as

well as NIH R35 CA232130 (JSL). PMRP acknowledges the Tow Foundation Postdoctoral Fellowship from the MSK Center for Molecular Imaging and Nanotechnology. AB is grateful to the Portuguese League Against Cancer for her Fellowship. RVU acknowledges support from the US Army Research 719 Office (proposal number 69180-CH). We thank Luca Gasperini for his help in the quantification of **NBDG** fluorescence images using the Cell Profiler software and Andreia Carvalho for providing comments and suggestions that were helpful in acquiring data for this manuscript.

Notes and references

1 WHO (WHO), *Latest global cancer data: Cancer burden rises to 18.1 million new cases and 9.6 million cancer deaths in 2018*, International Agency for research in cancer, 2018.
2 J. Zhou and B. Xu, *Bioconjugate Chem.*, 2015, **26**, 987–999.
3 R. A. Pires, Y. M. Abul-Haija, R. L. Reis, R. V. Ulijn and I. Pashkuleva, *Hydrogels: Design, Synthesis and Application in Drug Delivery and Regenerative Medicine*, 2018, p. 170.
4 D. Hanahan and R. A. Weinberg, *Cell*, 2011, **144**, 646–674.
5 R. A. Cairns, I. S. Harris and T. W. Mak, *Nat. Rev. Cancer*, 2011, **11**, 85–95.
6 Z. M. Yang, K. M. Xu, Z. F. Guo, Z. H. Guo and B. Xu, *Adv. Mater.*, 2007, **19**, 3152–3156.
7 R. A. Pires, Y. M. Abul-Haija, D. S. Costa, R. Novoa-Carballal, R. L. Reis, R. V. Ulijn and I. Pashkuleva, *J. Am. Chem. Soc.*, 2015, **137**, 576–579.
8 K. Kapoor, J. S. Finer-Moore, B. P. Pedersen, L. Caboni, A. Waight, R. C. Hillig, P. Bringmann, I. Heisler, T. Muller, H. Siebeneicher and R. M. Stroud, *Proc. Natl. Acad. Sci. U. S. A.*, 2016, **113**, 4711–4716.
9 D. A. Chan, P. D. Sutphin, P. Nguyen, S. Turcotte, E. W. Lai, A. Banh, G. E. Reynolds, J. T. Chi, J. Wu, D. E. Solow-Cordero, M. Bonnet, J. U. Flanagan, D. M. Bouley, E. E. Graves, W. A. Denny, M. P. Hay and A. J. Giaccia, *Sci. Transl. Med.*, 2011, **3**, 94ra70.
10 C. Granchi, S. Fortunato and F. Minutolo, *Medchemcomm*, 2016, **7**, 1716–1729.
11 J. Zhou, X. W. Du, N. Yamagata and B. Xu, *J. Am. Chem. Soc.*, 2016, **138**, 3813–3823.
12 Z. Q. Q. Feng, H. M. Wang, X. Y. Chen and B. Xu, *J. Am. Chem. Soc.*, 2017, **139**, 15377–15384.
13 Q. Yao, Z. Huang, D. Liu, J. Chen and Y. Gao, *Adv. Mater.*, 2018, **31**, 1804814.
14 D. Kalafatovic, M. Nobis, N. Javid, P. W. J. M. Frederix, K. I. Anderson, B. R. Saunders and R. V. Ulijn, *Biomater. Sci.*, 2015, **3**, 246–249.
15 D. Kalafatovic, M. Nobis, J. Y. Son, K. I. Anderson and R. V. Ulijn, *Biomaterials*, 2016, **98**, 192–202.
16 J. Son, D. Kalafatovic, M. Kumar, B. Yoo, M. A. Cornejo, M. Contel and R. V. Ulijn, *ACS Nano*, 2019, **13**, 1555–1562.
17 Y. Kuang, J. F. Shi, J. Li, D. Yuan, K. A. Alberti, Q. B. Xu and B. Xu, *Angew. Chem., Int. Ed.*, 2014, **53**, 8104–8107.
18 H. B. Shi, R. T. K. Kwok, J. Z. Liu, B. G. Xing, B. Z. Tang and B. Liu, *J. Am. Chem. Soc.*, 2012, **134**, 17972–17981.
19 C. F. Anderson and H. G. Cui, *Ind. Eng. Chem. Res.*, 2017, **56**, 5761–5777.
20 A. G. Cheetham, Y. A. Lin, R. Lin and H. G. Cui, *Acta Pharmacol. Sin.*, 2017, **38**, 874–884.
21 Y. Kuang and B. Xu, *Angew. Chem., Int. Ed.*, 2013, **52**, 6944–6948.
22 A. Brito, Y. M. Abul-Haija, D. S. da Costa, R. Novoa-Carballal, R. L. Reis, R. V. Ulijn, R. A. Pires and I. Pashkuleva, *Chem. Sci.*, 2019, **10**, 2385–2390.
23 L. S. Birchall, S. Roy, V. Jayawarna, M. Hughes, E. Irvine, G. T. Okorogheye, N. Saudi, E. De Santis, T. Tuttle, A. A. Edwards and R. V. Ulijn, *Chem. Sci.*, 2011, **2**, 1349–1355.
24 S. Rastogi, S. Banerjee, S. Chellappan and G. R. Simon, *Cancer Lett.*, 2007, **257**, 244–251.
25 A. Grosdidier, V. Zoete and O. Michielin, *Proteins: Struct., Funct., Bioinf.*, 2007, **67**, 1010–1025.
26 A. Grosdidier, V. Zoete and O. Michielin, *J. Comput. Chem.*, 2011, **32**, 2149–2159.
27 D. Deng, P. C. Sun, C. Y. Yan, M. Ke, X. Jiang, L. Xiong, W. L. Ren, K. Hirata, M. Yamamoto, S. L. Fan and N. Yan, *Nature*, 2015, **526**, 391–396.
28 D. Deng, C. Xu, P. C. Sun, J. P. Wu, C. Y. Yan, M. X. Hu and N. Yan, *Nature*, 2014, **510**, 121–125.
29 J. Barretina, G. Caponigro, N. Stransky, K. Venkatesan, A. A. Margolin, S. Kim, C. J. Wilson, J. Lehar, G. V. Kryukov, D. Sonkin, A. Reddy, M. W. Liu, L. Murray, M. F. Berger, J. E. Monahan, P. Morais, J. Meltzer, A. Korejwa, J. Jane-Valbuena, F. A. Mapa, J. Thibault, E. Bric-Furlong, P. Raman, A. Shipway, I. H. Engels, J. Cheng, G. Y. K. Yu, J. J. Yu, P. Aspesi, M. de Silva, K. Jagtap, M. D. Jones, L. Wang, C. Hatton, E. Palescandolo, S. Gupta, S. Mahan, C. Sougnez, R. C. Onofrio, T. Liefeld, L. MacConaill, W. Winckler, M. Reich, N. X. Li, J. P. Mesirov, S. B. Gabriel, G. Getz, K. Ardlie, V. Chan, V. E. Myer, B. L. Weber, J. Porter, M. Warmuth, P. Finan, J. L. Harris, M. Meyerson, T. R. Golub, M. P. Morrissey, W. R. Sellers, R. Schlegel and L. A. Garraway, *Nature*, 2012, **483**, 603–607.
30 N. Stransky, M. Ghandi, G. V. Kryukov, L. A. Garraway, J. Lehar, M. Liu, D. Sonkin, A. Kauffmann, K. Venkatesan, E. J. Edelman, M. Riester, J. Barretina, G. Caponigro, R. Schlegel, W. R. Sellers, F. Stegmeier, M. Morrissey, A. Amzallag, I. Pruteanu-Malinici, D. A. Haber, S. Ramaswamy, C. H. Benes, M. P. Menden, F. Iorio, M. R. Stratton, U. McDermott, M. J. Garnett, J. Saez-Rodriguez and C. Drug Sensitivity, L. Cancer Cell, I. Broad, R. Novartis Inst Biomed, S. Genomics Drug, H. Massachusetts Gen, L. European Mol Biol, I. European Bioinformatics and I. Wellcome Trust Sanger, *Nature*, 2015, **528**, 84–87.
31 K. Yamada, M. Nakata, N. Horimoto, M. Saito, H. Matsuoka and N. Inagaki, *J. Biol. Chem.*, 2000, **275**, 22278–22283.
32 C. H. Zou, Y. J. Wang and Z. F. Shen, *J. Biochem. Biophys. Methods*, 2005, **64**, 207–215.
33 K. Yamada, M. Saito, H. Matsuoka and N. Inagaki, *Nat. Protoc.*, 2007, **2**, 753–762.

34 P. Hein, M. C. Michel, K. Leineweber, T. Wieland, N. Wettschureck and S. Offermanns, in *Practical Methods in Cardiovascular Research*, ed. S. Dhein, F. Wilhelm Mohr and M. Delmar, Springer, Berlin, Heidelberg, 2005, ch. 6, pp. 723–783, DOI: 10.1007/b137833.
35 F. J. Lopez-Hernandez, M. A. Ortiz, Y. Bayon and F. J. Piedrafita, *Mol. Cancer Ther.*, 2003, **2**, 255–263.
36 N. Takahashi, L. Duprez, S. Grootjans, A. Cauwels, W. Nerinckx, J. B. DuHadaway, V. Goossens, R. Roelandt, F. Van Hauwermeiren, C. Libert, W. Declercq, N. Callewaert, G. C. Prendergast, A. Degterev, J. Yuan and P. Vandenabeele, *Cell Death Dis.*, 2012, **3**, 891–899.
37 Y. Q. Wu, D. Zhao, J. N. Zhuang, F. Q. Zhang and C. Xu, *PLoS One*, 2016, **11**, e0168268.
38 F. Pirnia, E. Schneider, D. C. Betticher and M. M. Borner, *Cell Death Differ.*, 2002, **9**, 905–914.
39 R. A. Gatenby and R. J. Gillies, *Nat. Rev. Cancer*, 2004, **4**, 891–899.
40 P. P. Hsu and D. M. Sabatini, *Cell*, 2008, **134**, 703–707.
41 M. L. Macheda, S. Rogers and J. D. Best, *J. Cell. Physiol.*, 2005, **202**, 654–662.
42 J. Zhou, X. W. Du and B. Xu, *Angew. Chem., Int. Ed.*, 2016, **55**, 5770–5775.

